Pure Appl. Chem., Vol. 83, No. 11, pp. 2107–2113, 2011.
doi:10.1351/PAC-CON-11-01-13

Metal-semiconductor-metal (MSM) photodetectors with plasmonic nanogratings*

Narottam Das[1,‡], Ayman Karar[1], Chee Leong Tan[2], Mikhail Vasiliev[1], Kamal Alameh[1,3,‡], and Yong Tak Lee[2,3]

[1]Electron Science Research Institute, Edith Cowan University, Joondalup, WA 6027, Australia; [2]Department of Information and Communications, Gwangju Institute of Science and Technology (GIST), 261 Cheomdan-gwagiro (Oryong-dong), Buk-gu, Gwangju, 500-712, Korea; [3]Department of Nanobio Materials and Electronics, GIST, Korea

Abstract: We discuss the light absorption enhancement factor dependence on the design of nanogratings inscribed into metal-semiconductor-metal photodetector (MSM-PD) structures. These devices are optimized geometrically, leading to light absorption improvement through plasmon-assisted effects. Finite-difference time-domain (FDTD) simulation results show ~50 times light absorption enhancement for 850 nm light due to improved optical signal propagation through the nanogratings. Also, we show that the light absorption enhancement is strongly dependent on the nanograting shapes in MSM-PDs.

Keywords: finite-difference time-domain (FDTD) simulation; magnetic properties; metal-semiconductor-metal (MSM) nanocomposites; nanocrystals; nanomaterials; nanophotonics; nanostructured materials; photodetectors; plasmonic nanogratings; surface plasmon.

INTRODUCTION

In recent years, sub-wavelength nanogratings have been recognized as promising candidates for realizing high-speed metal-semiconductor-metal photodetectors (MSM-PDs). Such nanogratings interact strongly with the incident light and potentially trap it inside the subsurface region of semiconductors [1]. MSM-PDs have extensive applications, including optical fiber communications and optical interconnects.

An MSM-PD contains interdigitated metal fingers deposited onto a semiconductor substrate. The interdigitated electrodes in MSM-PDs result in an enormous increase in bandwidth and decrease in dark current, in comparison with conventional PIN photodiodes with active areas of similar size [2]. Recently, the use of surface plasmon-assisted effects for the design of such photodetectors has been reported for the development of MSM-PDs having a high responsivity-bandwidth product, well beyond that of conventional PIN photodetectors, therefore attracting a great deal of interest [3]. In the past decade, there have been several theoretical and experimental research activities reported on the extraordinary optical transmission through the sub-wavelength metallic apertures [4,5] and periodic metal grating structures [6,7]. Finite-difference time-domain (FDTD) simulation results have shown signifi-

*Paper based on a presentation made at the International Conference on Nanomaterials and Nanotechnology (NANO-2010), Tiruchengode, India, 13–16 December 2010. Other presentations are published in this issue, pp. 1971–2113.
‡Corresponding authors: E-mail: k.alameh@ecu.edu.au and n.das@ecu.edu.au

cant enhancement of light absorption through interaction with surface plasmon polaritons (SPPs), and this has direct application to the design of MSM-PDs [1–4].

In this paper, we use the FDTD analysis to optimize a novel MSM-PD structure employing a single metal layer deposited onto a GaAs substrate and a nanograting etched into this layer. Our simulation results show that enhancement in light trapping near 850 nm of up to ~50 times is possible in comparison with conventional MSM-PDs. In particular, we investigate the degradation in absorption enhancement of practical nanogratings, which have trapezoidal, rather than rectangular, profiles after lithography or focused ion beam (FIB) milling.

DESIGN OF MSM-PD STRUCTURE

Figure 1 shows a novel MSM-PD structure, which consists of three separate layers, namely, (1) top layer: metal nanograting, (2) middle layer: unperturbed metal layer (underlayer) containing conventional sub-wavelength apertures, and (3) bottom layer: semiconductor (GaAs) substrate. The metal nanograting is formed by FIB milling the lines inside the gold (Au) layer with the grooves being perpendicular to the x-axis, and its dimensions and geometry are optimized to in-couple light near the design wavelength and trigger SPPs propagating along the z-axis. For a metal nanograting period of Λ, the wave vector of the excited SPPs is given in [1]

$$k_{sp} = \frac{\omega}{c}\sin\theta \pm \frac{2\pi l}{\Lambda} = \frac{\omega}{c}\sqrt{\frac{\varepsilon_m^{'}\varepsilon_d}{\varepsilon_m^{'}+\varepsilon_d}} \tag{1}$$

where ω is the angular frequency of the incident light wave, c is the speed of light in vacuum, θ is its angle of incidence with respect to the device normal, and l is an integer number, i.e., l = 1, 2, 3, ….. N. In our analysis, we denote the complex dielectric permittivity of the metal as $\varepsilon_m = \varepsilon_m^{'} + i\varepsilon_m^{''}$, where $\varepsilon_m^{'}$ and $\varepsilon_m^{''}$ are the real and imaginary part of the dielectric permittivity, respectively, $i = \sqrt{-1}$, and the dielectric permittivity of air (or the incidence medium) is denoted as ε_d. Therefore, the metal nanograting with a period Λ is required to match the surface plasmons' wavevector to that of the normally incident light ($\theta = 0$) of the angular frequency ω. Using eq. 1 to design the absorption enhancement peak spectrally located near 850 nm for the Au grating/Au/GaAs material system and air as incidence medium, we found that a grating periodicity of Λ = 810 nm was optimum. A single grating period contains a metal nanograting and a cut-out (free space) with a duty cycle of 50 % [1]. Several types of nanograting groove shape designs, shown in Fig. 1, were considered and specifically, the dependency of the plasmon-assisted light absorption enhancement on the geometric shape of the nanograting corrugations cross-sections was investigated using the FDTD analysis.

Figure 1a shows a schematic diagram of an MSM-PD with plasmonic rectangular-shaped metal nanogratings etched inside the top part of the Au layer. The thickness of the unperturbed metal layer containing sub-wavelength apertures is shown as h_s, the height of the metallic nanogratings h_g, and the sub-wavelength aperture width is x_w.

Figure 1b shows a trapezoidal-shaped metal nanograting profile that was used for the simulation. It is the closest cross-sectional profile to that developed using FIB lithography in the case of small-feature-size (sub-100 nm) nanopatterned grooves. Figure 1c shows a triangular-shaped metal nanograting profile.

Figures 1a–c all show that a metal (Au) layer is deposited on top of the semiconductor (GaAs) substrate; the thickness of this layer was kept constant at 100 nm throughout the analysis. In the simulation, a range of grating profile-shape variations was considered, keeping the unperturbed part of metal layer (underlayer) thickness at 10 nm and the metal nanograting height h_g at 90 nm. The light is normally incident on top of the plasmonic nanograting.

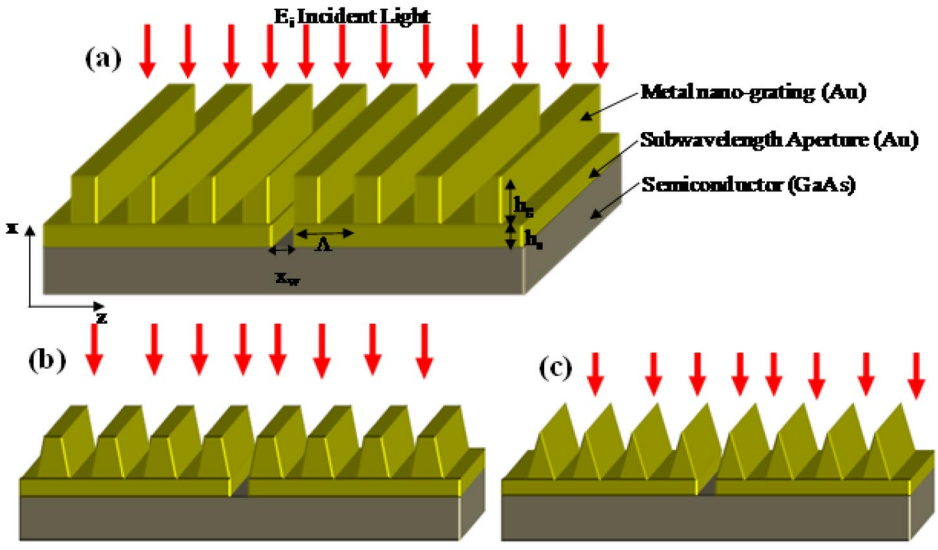

Fig. 1 Schematic diagrams of several MSM-PD structures with metal nanogratings etched inside the top part of the Au layer. The metal nanograting profiles are: (a) rectangular-shaped, (b) trapezoidal-shaped, and (c) triangular-shaped.

Figures 2a,b show a scanning electron microscopy (SEM) image of the plasmonic metal nanograting etched inside the top part of the Au layer using the FIB milling process. From SEM imaging, it was found that the FIB milling was better than conventional photolithography processes for cutting sharp-edge profiles. Furthermore, the atomic force microscopy (AFM) images showed that the nanograting's profile is trapezoidal rather than rectangular. The trapezoidal groove shape is formed due to the re-deposition of the etched Au atoms and the truncation of nanograting edges due to the ion beam. Figure 2c shows the AFM image and confirmed the shape of the nanograting is close to the trapezoidal profiles. Based on these experimental results, the shape of the nanograting was taken into account in the simulation of the shape dependency of light absorption enhancement in MSM-PDs.

The incident light normally passes through the sub-wavelength apertures and reaches into the GaAs substrate, and therefore, generates electron-hole pairs. In addition, the light absorption within GaAs is assisted by the SPPs excited near the metal-semiconductor interface in the nanograting regions. The energy of light incident on the metal nanograting is coupled partially into propagating SPPs that can improve the light absorption efficiency in thin sub-surface regions of semiconductor under the sub-wavelength apertures. The improvement of light absorption of the nanograting is due to SPP-generated localized regions of high-intensity electric field distribution (as shown in Fig. 3). So, the nanograting acts as light concentrators (plasmonic lenses) or collectors, which is necessary for triggering the extraordinary optical absorption (EOA) of light within the active regions of photodetectors. Two-dimensional FDTD models of several groove shape designs of MSM-PDs (with and without the metal nanograting) were generated using Opti-FDTD software package developed by Optiwave, Inc. In the simulation, we used a mesh step size of $\delta x = 5$ nm and a time step of $\delta t < 0.1\delta x/c$. The excitation field was modeled as a Gaussian-modulated continuous wave. The incident light wave was TM-polarized (its electric field oscillation direction was along the z-axis, perpendicular to the nanograting grooves). The anisotropic perfectly matched layer (APML) boundary conditions were applied in both x- and z-directions. The Au dielectric permittivity was defined by the Lorentz–Drude model [8], and the dielectric permittivity data of GaAs was taken from [9].

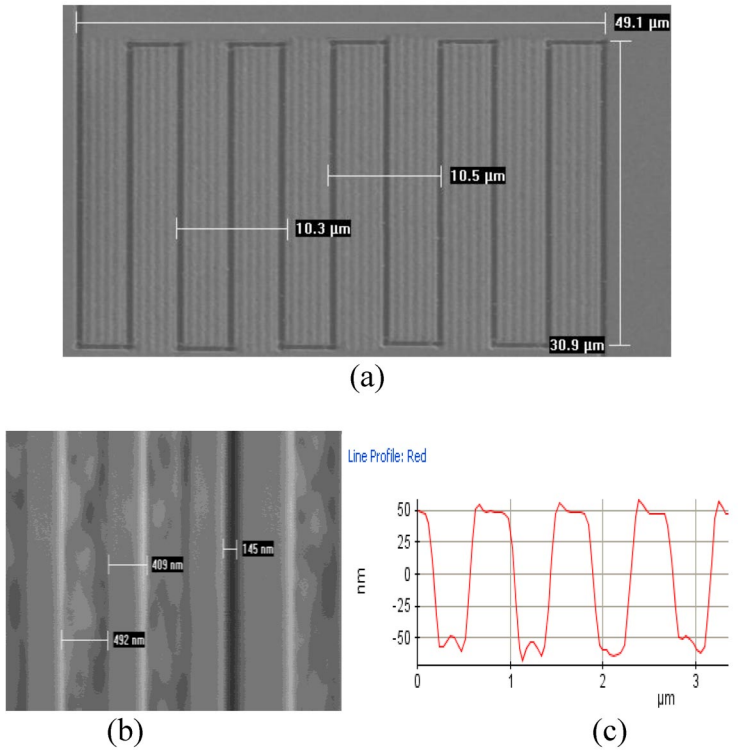

Fig. 2 Experimental results: (a) a typical SEM image of the nanograting fabricated with FIB lithography process, (b) a detailed image of a portion of the fabricated nanograting, and (c) AFM image of the fabricated nanograting profile.

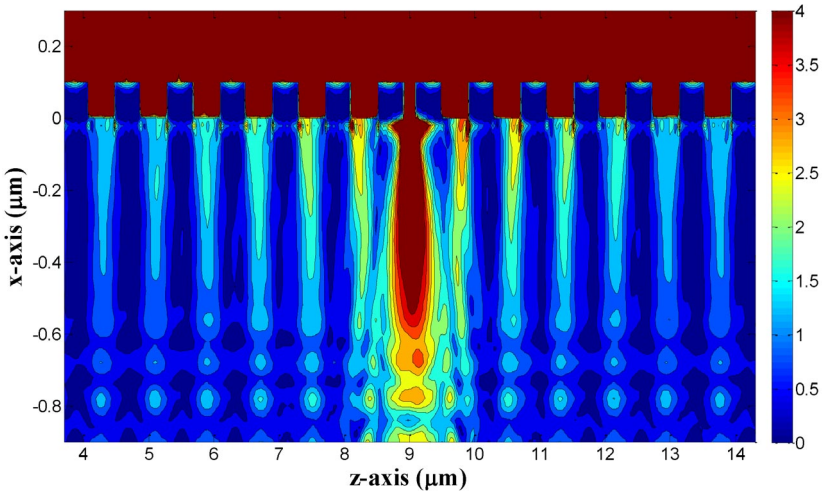

Fig. 3 Total electric field intensity distribution in the cross-section of computational volume behind the nanograting with rectangular grooves cross-section and the following grating parameters: the nanograting height is 90 nm, unperturbed Au layer thickness is 10 nm, grating period is 810 nm, and the sub-wavelength aperture width is 150 nm. The color scale has been optimized for representing small weak-field intensity variations.

A density plot of the total (transmitted) electric field strength within the substrate cross-section is shown in Fig. 3. We used a custom-designed Matlab algorithm to compute the total electric field intensity distribution, as a result of vector summation of the modeled complex electric field component distributions along the x-direction (E_x) and z-direction (E_z). It is clearly observed in Fig. 3 that the significant amount of light is passing through the region of sub-wavelength aperture width is mainly due to the plasmon-assisted effects, which result in propagating SPPs excited by the incident light waves and the energy concentration (by plasmonic lenses) within small material volumes near the photodetector's active region.

RESULTS AND DISCUSSION

In this section, we discuss the simulation results of different MSM-PD structures having several types of nanograting groove-geometry designs and the light absorption enhancement dependency on the sub-wavelength aperture width. We particularly modeled the nanograting groove-shape dependency and the aperture width dependency of the light absorption enhancement factor, defined as the ratio of the normalized power transmittance of an MSM-PD with metal nanograting to the normalized power transmittance of a similar MSM-PD without metal nanograting [4]. The propagation of light through both MSM-PD structures of the described type was modeled for a range of sub-wavelength aperture widths whilst keeping the values of h_s = 10 nm and h_g = 90 nm (optimized separately for devices operating near the wavelength 830 nm) constant.

Figure 4 shows the simulated light absorption enhancement factor spectra of several optimized MSM-PD structures. For this case, the grooves of the nanograting are rectangular-shaped in their cross-section. We varied the sub-wavelength aperture widths between 50–200 nm. The results show that the light absorption enhancement factor decreases rapidly with the increasing of sub-wavelength aperture widths. The light enhancement factor is ~50 times for 50-nm-wide sub-wavelength aperture width and ~17 times for 200 nm aperture width. The simulation results shown in Fig. 4 are in excellent agreement with the results reported in ref. [10], therefore validating the FDTD simulation model used in this paper.

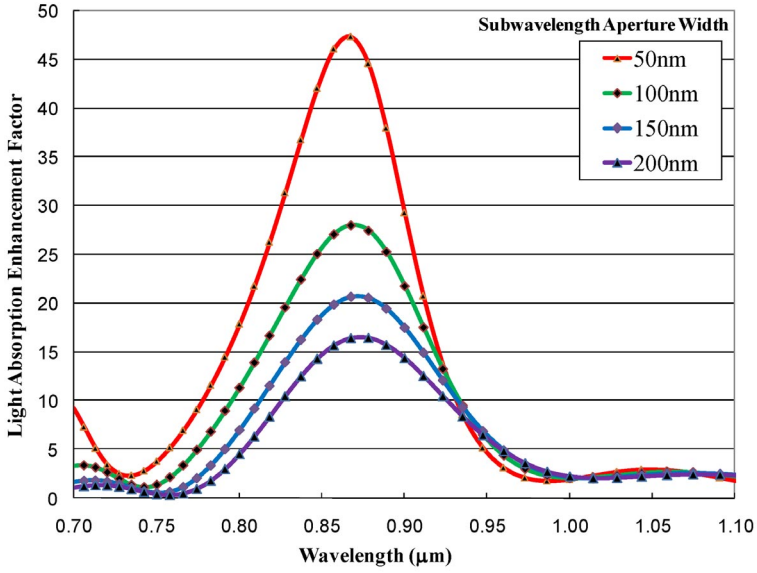

Fig. 4 Light absorption enhancement factor spectra for MSM-PDs with plasmon-assisted operation. Here, the sub-wavelength aperture widths were varied between 50–200 nm, and all the groove shapes were rectangular-profile.

The spectral distribution of the light absorption enhancement factor for different nanograting groove shapes are shown in Fig. 5. For this simulation, the aperture width was kept constant at 50 nm. We modeled the effects of different types of nanograting groove geometries on light propagation and obtained the following results. These are: (a) the predicted light absorption enhancement factor was at its maximum ~50 times for a rectangular-shaped nanograting, and (b) the absorption enhancement factor was reduced progressively with the decreasing aspect ratios (trapezoid-top to base length ratios) for the trapezoidal-shaped nanograting. For the trapezoidal-shaped profile with the aspect ratio of 0.9, the light enhancement factor was reduced ~30 % compared to its "ideal-case" maximum. We also simulated the light absorption enhancement factor for the aspect ratios of 0.7, 0.5, and 0.2 as shown in Fig. 5. So, this groove-shape dependency of light absorption enhancement is the primary importance in practical manufacturing situations. In addition, the triangular-shaped nanograting groove geometry has shown in Fig. 5 results in light absorption enhancement of only 5 times.

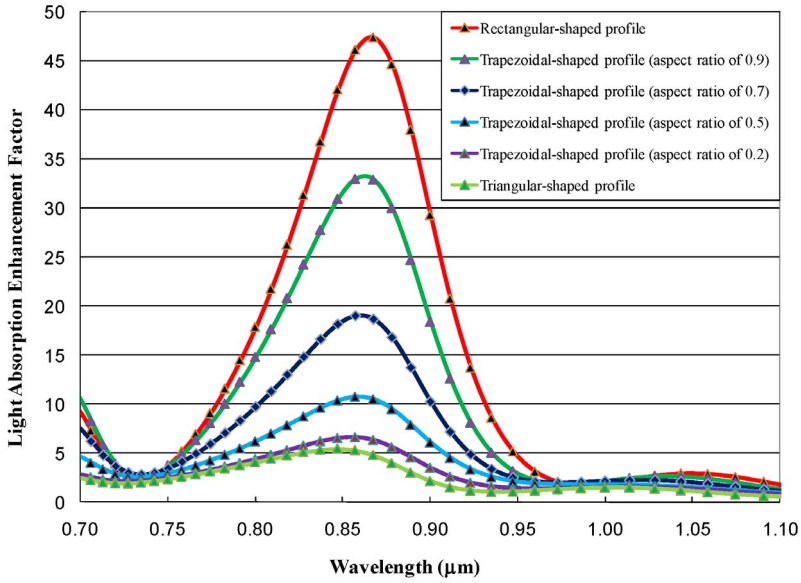

Fig. 5 Light absorption enhancement factor spectra for different nanograting groove shapes. In this case, the subwavelength aperture width was kept constant at 50 nm.

CONCLUSIONS

We have modeled the light-capture performance of novel MSM-PD structures employing metal nanogratings of different cross-sectional shapes in terms of the light absorption enhancement and hence the responsivity-bandwidth products. The simulation results have shown that the novel MSM-PD structures can attain a maximum light absorption enhancement near 850 nm of almost 50 times (when the nanograting shape is rectangular) better than the conventionally designed MSM-PDs. Also, we have analyzed the reality of different metal nanograting groove shapes for practical device manufacturing considerations. We found that the light absorption enhancement is strongly dependent on the nanograting shapes in MSM-PDs. The results reported are useful for the design and development of MSM-PDs with high responsivity-bandwidth products.

ACKNOWLEDGMENTS

The authors acknowledge the support of the Faculty of Computing Health and Science, Edith Cowan University, Australia, and the Department of Nano-bio Materials and Electronics, Gwangju Institute of Science and Technology, Republic of Korea.

REFERENCES

1. J. A. Shackleford, R. Grote, M. Currie, J. E. Spanier, B. Nabet. *Appl. Phys. Lett.* **94**, 083501 (2009).
2. J. B. D. Soole, H. Schumacher. *IEEE J. Quantum Electron.* **27**, 737 (1991).
3. J. Hetterich, G. Bastian, N. A. Gippius, S. G. Tikhodeev, G. von Plessen, U. Lemmer. *IEEE J. Quantum Electron.* **43**, 855 (2007).
4. C. L. Tan, V. V. Lysak, K. Alameh, Y. T. Lee. *Opt. Commun*. **283**, 1763 (2010).
5. G. Lévêque, O. J. F. Martin, J. Weiner. *Phys. Rev. B* **76**, 155418 (2007).
6. F. J. García-Vidal, H. J. Lezec, T. W. Ebbesen, L. Martín-Moreno. *Phys. Rev. Lett.* **90**, 213901 (2003).
7. H. J. Lezec, T. Thio. *Opt. Express* **12**, 3629 (2004).
8. A. D. Rakić, A. B. Djurišić, J. M. Elazar, M. L. Majewski. *Appl. Opt.* **37**, 5271 (1998).
9. E. D. Palik. "Galllium arsenide (GaAs)", in: *Handbook of Optical Constants of Solids*, E. D. Palik (Ed.), Academic, San Diego (1985).
10. J. S. White, G. Veronis, Z. Yu, E. S. Barnard, A. Chandran, S. Fan, M. L. Brongersma. *Opt. Lett.* **34**, 686 (2009).

